E-DNA Sensor of Mycobacterium tuberculosis Based on Electrochemical Assembly of Nanomaterials (MWCNTs/PPy/PAMAM)

ARTICLE *in* ANALYTICAL CHEMISTRY · AUGUST 2015

Impact Factor: 5.64 · DOI: 10.1021/acs.analchem.5b01761 · Source: PubMed

5 AUTHORS, INCLUDING:

Anna Miodek
Atomic Energy and Alternative Energies Com…
18 PUBLICATIONS **74** CITATIONS
SEE PROFILE

Michel Kiréopori Gomgnimbou
Université Paris-Sud 11
22 PUBLICATIONS **82** CITATIONS
SEE PROFILE

Hafsa Korri-Youssoufi
Université Paris-Sud 11
80 PUBLICATIONS **1,419** CITATIONS
SEE PROFILE

analytical chemistry

Article

pubs.acs.org/ac

E-DNA Sensor of *Mycobacterium tuberculosis* Based on Electrochemical Assembly of Nanomaterials (MWCNTs/PPy/PAMAM)

Anna Miodek,[†] Nawel Mejri,[†] Michel Gomgnimbou,[‡] Christophe Sola,[‡] and Hafsa Korri-Youssoufi*[,†]

[†]CNRS UMR-8182, Institut de Chimie Moléculaire et de Matériaux d'Orsay, Equipe de Chimie Bioorganique et Bioinorganique, Université Paris-Sud, Bâtiment 420, 91405 Orsay, France

[‡]Institut of Integrative Cell Biology, Orsay, CEA-CNRS-Université Paris-Sud, UMR9198, Bâtiment 400, 91405 Orsay, France

Supporting Information

ABSTRACT: Two-step electrochemical patterning methods have been employed to elaborate composite nanomaterials formed with multiwalled carbon nanotubes (MWCNTs) coated with polypyrrole (PPy) and redox PAMAM dendrimers. The nanomaterial has been demonstrated as a molecular transducer for electrochemical DNA detection. The nanocomposite MWCNTs-PPy has been formed by wrapping the PPy film on MWCNTs during electrochemical polymerization of pyrrole on the gold electrode. The MWCNTs-PPy layer was modified with PAMAM dendrimers of fourth generation (PAMAM G4) with covalent bonding by electro-oxidation method. Ferrocenyl groups were then attached to the surface as a redox marker. The electrochemical properties of the nanomaterial (MWCNTs-PPy-PAMAM-Fc) were studied using both square wave voltammetry and cyclic voltammetry to demonstrate efficient electron transfer. The nanomaterial shows high performance in the electrochemical detection of DNA hybridization leading to a variation in the electrochemical signal of ferrocene with a detection limit of 0.3 fM. Furthermore, the biosensor demonstrates ability for sensing DNA of *rpoB* gene of *Mycobacterium tuberculosis* in real PCR samples. Developed biosensor was suitable for detection of sequences with a single nucleotide polymorphism (SNP) T (TCG/TTG), responsible for resistance of *M. tuberculosis* to rifampicin drug, and discriminating them from wild-type samples without such mutation. This shows potential of such systems for further application in pathogens diagnostic and therapeutic purpose.

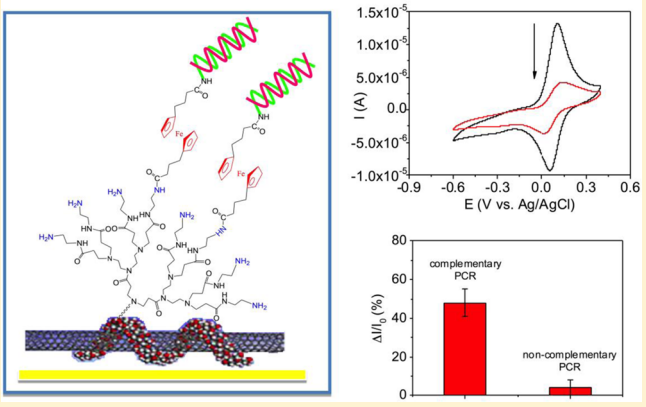

Nanostructures, such as carbon nanotubes (CNTs), have been extensively used as transducers for electrochemical biosensing analysis.[1] These nanomaterials offer a large surface-to-volume ratio and exhibit excellent chemical and thermal stability.[2] Moreover, they have electronic properties leading to the enhancement of electron transport. Thus, multiwalled carbon nanotubes (MWCNTs) are appropriate nanomaterials for covalent binding of redox proteins and mediators.[3]

One of the challenges with employing CNTs in a biosensor device is their inefficient immobilization on the surface to individually disperse nanotubes. CNTs are insoluble in aqueous and polar media and have a tendency to form agglomerates due to hydrophobic interactions and van der Waals forces between nanotubes. Different methods have been developed for this purpose, such as adsorption on the electrode by drop casting,[4] self-assembled incorporation,[5] covalent grafting to modified electrodes,[6,7] or their direct synthesis on the surface.[8] Entrapment in conductive organic polymers (COPs)[9,10] are useful methods for CNTs immobilization as COPs could bring additional properties, such as mechanical or electrical, as demonstrated in the case of CNTs/polypyrrole[11,12] and CNTs/polyaniline.[13] Another challenge in the development of CNTs-based biosensor devices is their modification by bioreceptors, which can be achieved through chemical attachment of biomolecules to the carboxylic groups of modified CNTs.[14] Recent trends are based on the association of CNTs with others nanomaterials such as dendrimers.[15] The poly(amidoamine) dendrimers of fourth generation (PAMAM G4) possess 64 primary amine groups on the surface[16,17] and have been successfully applied in the fabrication of DNA biosensors.[18,19] Because of the high number of amines groups on the dendrimers' surface, it easily associates with a large number of bioreceptors, increasing the sensitivity and detection limit of the target. The PAMAM G4 dendrimers can be covalently attached to the carboxylic acid of modified MWCNTs through an amide link and the resultant nanomaterial can then be applied as a platform for electrochemical detection.[20] We demonstrated previously that high surface coverage of CNTs or PPy with redox PAMAM improves

Received: May 11, 2015
Accepted: July 29, 2015

DOI: 10.1021/acs.analchem.5b01761
Anal. Chem. XXXX, XXX, XXX−XXX

sensitivity and provides increased dynamic range during detection.[20,21]

In this work, we demonstrated for the first time that association of these nanomaterials (PPy, MWCNTs, and PAMAM G4) can be achieved through a simple two-step method following electrochemical patterning which could be performed in very short time, less than 5 min. The resultant nanomaterial can be used as transducer for electrochemical DNA detection in complex matrix such as PCR samples and can discriminate the mismatch bases of DNA from drug resistant *Mycobacterium tuberculosis*. Additionally, wrapping of MWCNTs with PPy film and further functionalization with PAMAM G4 on the surface can lead to avoid nonspecific interaction that could be obtained between MWCNTs and DNA.

The warping reaction was performed during electrochemical polymerization of pyrrole in solution containing CNTs allowing their deposition on gold surface in a controlled and reproducible way. The modification of the composite with PAMAM G4 dendrimers was then achieved through the electrochemical oxidation of amine groups, resulting in covalent attachment to the MWCNTs-PPy surface. In order to obtain intense electrochemical signal, redox marker, ferrocene[22,23] functionalized with two activated carboxylic groups was then covalently bonded via the amide link giving MWCNTs-PPy-PAMAM-Fc. Binding of the ssDNA probe for biosensor construction was done by covalent attachment through DNA modified by amine group on its 5′-end position. DNA hybridization studies were performed with complementary (from 1 fM to 100 nM) and noncomplementary (1 μM) targets. We demonstrated that this method allows fabrication of a homogeneous layer of MWCNTs-PPy-PAMAM and such nanomaterial allows DNA detection via ferrocene signal with high sensitivity and specificity and could be applied for detection of biological samples such as DNA from *Mycobacterium tuberculosis* strains.

EXPERIMENTAL SECTION

Reagents. All synthetic DNA sequences were provided by Eurogentec company (Eurogentec, Liège, Belgium). The DNA probe was a 15-bases sequence with six carbon chains (C6) as spacer and with amine group on its 5′ phosphoryl terminus: NH_2-C6-5′GAT-ACT-TCT-ATC-ACC3′. The sequences of 15-bases and 75-bases targets specific to the DNA probe were 5′GGT-GAT-AGA-AGT-ATC3′ and 5′GGT-GAT-AGA-AGT-ATC-CCG-AGC-TTG-AGA-TCT-TCT-GCG-ACG-CGG-CGA-TTG-AGA-CCT-TCG-TCT-GCG-AGG-CGA-GGG3′, respectively. The noncomplementary 14-bases oligonucleotide was 5′CAT-TCC-CTC-TTA-GG3′.

The DNA probe specific to the *Mycobacterium tuberculosis* PCR products (411 bp) was provided from IDT^R company (Leuven, Integrated DNA Technologies, BVBA, Interleuvenlaan 12A B-3001 Leuven, Belgium), contained 18 bases and was modified with 12 carbonyl chain (C12) bearing an amine group at the terminal position: NH_2-C12-5′CCG-ACT-GTT-GGC-GCT-GGG3′. This probe (for *M. tuberculosis*) targets specifically the mutant single nucleotide polymorphism (SNP) T (TCG/TTG) in the codon position 531 of *rpoB* gene conferring resistance of *M. tuberculosis* to rifampicin drug. The wild-type codon is TCG and the targeted mutant codon by the probe is TTG. For information about PCR products and amplification procedure see Supporting Information, Experimental Section.

The description of reagents 1,1′-(phtalimide butanoate) ferrocene Fc$(NHP)_2$, MWCNTs, pyrrole and PAMAM G4 dendrimers is described in the Supporting Information (Experimental Section).

Entrapment of MWCNTs in Polypyrrole Film. MWCNTs were dissolved by sonication in H_2O containing 0.5 M $LiClO_4$ and mixed with pyrrole (Py) monomers with the following concentrations: 1 mg·mL^{-1} for MWCNTs and 0.1 M for pyrrole. The MWCNTs coated with polypyrrole film (MWCNTs-PPy) was grown on the gold surface by cycling the potential from −0.4 to 0.9 V vs Ag/AgCl with scan rate of 100 mV·s^{-1} during 2 cycles. The number of cycles and range of potential were optimized. During the electropolymerization, the working and counter electrode were separated in a small-volume cell (Basi) containing the solution of MWCNTs and pyrrole. Following the reaction, the electrode was rinsed several times with double-distilled water.

Association of PAMAM G4 Dendrimers. PAMAM G4 dendrimers were immobilized on the MWCNTs-PPy layer by covalent bonding through electro-oxidation of amine groups of PAMAM G4. Electrodeposition was performed in H_2O containing 50 μM PAMAM G4 and 0.5 M $LiClO_4$ by scanning the potential from 0.0 to 1.1 V vs Ag/AgCl for 3 cycles with a scan rate of 50 mV·s^{-1}. The reaction was performed in a small volume cell similar to that described for electropolymerization.

Association of Ferrocene and DNA Probe. Covalent bonding of ferrocene, modified by two phtalymidyl Fc$(NHP)_2$ was performed by immersing the modified MWCNTs-PPy-PAMAM electrode into a solution of 1 mM ferrocene prepared in acetonitrile for 1 h at room temperature, around 22 °C. The time and concentration of ferrocene were optimized to obtain a suitable number of ferrocenyl groups attached to the surface, ensuring significant variation of the redox signal during detection of the complementary target. Unbound residues were washed by acetonitrile and double-distilled water. The electrode was then immersed in 10 mM solution of ssDNA probe and incubated for 1 h at room temperature, around 22 °C. The electrode was then rinsed with double-distilled water and PBS buffer. To saturate all unbound phtalymidyl esters of ferrocene and to avoid nonspecific interactions of the DNA target with dendrimers, the electrode was then immersed in 1 mM ethanolamine (EtOH) solution in PBS buffer for 30 min at room temperature. Finally, the biosensor was carefully washed with double-distilled water and PBS buffer and stored in PBS buffer at 4 °C overnight.

Hybridization with Complementary Target. The hybridization of complementary ssDNA targets of 15- and 75-bases with the ssDNA probe immobilized on the surface was performed by incubating the modified electrode in a solution of the DNA target for 1 h at 37 °C. Hybridization with the following concentrations of DNA target were studied: 1, 10, 100 fM; 1, 10, 100 pM; 1, 10, 100 nM. After incubation, the electrode was carefully washed with double-distilled water and PBS buffer. Nonspecific interactions were tested by immersing the electrode in 1 μM of noncomplementary targets in PBS buffer and incubated in the same conditions as those for the complementary target. The same conditions were also used for the detection of DNA from PCR samples. Before reaction with biosensor, DNA from PCR samples was denaturized by heating at 95 °C for 4 min.

The instrumentation used in this work is described in the Supporting Information, in the Experimental Section.

DOI: 10.1021/acs.analchem.5b01761
Anal. Chem. XXXX, XXX, XXX−XXX

Scheme 1. Schematic Representation of the Various Steps of Biosensor Formation Based on MWCNTs Coated with PPy, PAMAM G4 Dendrimers, and Ferrocene for DNA Detection[a]

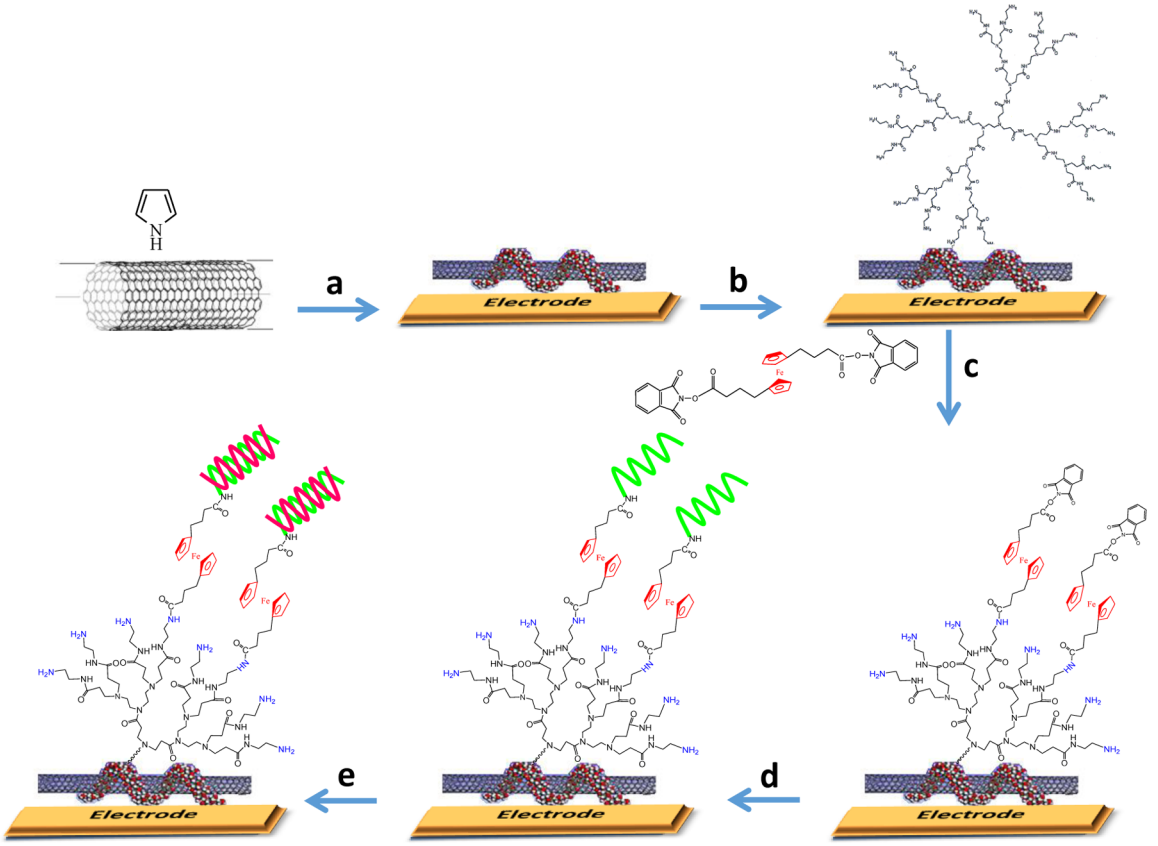

[a]Step a: electropolymerization by cycling potential from −0.4 to 0.9 V. Step b: Dendrimers attachment through electrochemical oxidation of PAMAM's G4 amines. Step c: Covalent attachement of ferrocene by dipping the electrode in solution of modified ferrocene. Step d: Covalent attachment of DNA, bearing amine in 5′ position, in PBS at room temperature. Step e: Hybridization reaction of the DNA target by dipping the electrode in PBS buffer solution containing the DNA target for 1 h at 37 °C.

RESULTS AND DISCUSSION

Formation of Nanocomposite and Characterizations.

All steps of biosensor construction are presented on Scheme 1.

Wrapping of polypyrrole film on carboxylated MWCNTs was performed in solution containing both pyrrole monomers and oxidized CNTs by electrochemical scanning of the potential. Various experimental conditions have been studied such as concentration of pyrrole monomer and CNTs; the potential range; and the number of scans. The optimal conditions for coating the electrode surface with a homogeneous layer of MWCNTs-PPy were chosen as 1 mg·mL^{-1} of MWCNTs in 100 mM of pyrrole monomer solution, scanning the potential between −0.4 and 0.9 V for 2 cycles. The nanocomposite was first characterized by cyclic voltammetry (CV) in the presence of a redox marker $[Fe(CN)_6]^{4-}$/$[Fe(CN)_6]^{3-}$ to demonstrate the effect of the electrode modification with MWCNTs-PPy (see Figure S-1). This analysis demonstrates that such nanomaterial increases the active surface of the modified electrode and that electrochemical polymerization allows the efficient association of MWCNTs-PPy to the electrode surface with high reproducibility in a very short time compared to an adsorption of nanotubes by drop casting.

Dendrimers immobilization on MWCNTs-PPy was performed by electrochemical pattering to provide functional groups on the surface for further functionalization with bioreceptors. The modification was performed through oxidation of amine groups of PAMAM G4 (see Supporting Information S-2.2 and Figure S-2). The oxidation of amine groups of PAMAM G4 leads to the formation of radicals that attach to the aromatic rings of the MWCNTs-PPy layer by covalent bonding. The covalent attachment of amines through electro-oxidation onto the surface of the glassy carbon electrode or CNTs was demonstrated previously through oxidation of linear chains such as ethylene diamine.[24−26] The reaction mechanism assumes that oxidized amines in radical forms can react with aromatic groups of carbon surfaces resulting in the rupture of the C═C bond and formation of C−N link. The reaction of PAMAM G4 dendrimers with the MWCNTs-PPy composite assumes a covalent bonding of electro-oxidized amines with the aromatic C═C present in carbon nanotubes as well as in polypyrrole. To confirm this association, some characterizations such as SEM, FT-IR and XPS have been performed on surfaces modified with MWCNTs-PPy and MWCNTs-PPy-PAMAM.

SEM images show surface modified with MWCNTs-PPy and MWCNTs-PPy-PAMAM compared to surface modified with PPy or carboxylated MWCNTs (see Figure 1). Gold-MWCNTs layer shows smooth surface due to CNTs with a diameter of 20−25 nm (Figure 1A). However, Gold-PPy layer demonstrates a typical morphology of "cauliflower" structure which is commonly obtained for polypyrrole formed in aqueous

DOI: 10.1021/acs.analchem.5b01761
Anal. Chem. XXXX, XXX, XXX−XXX

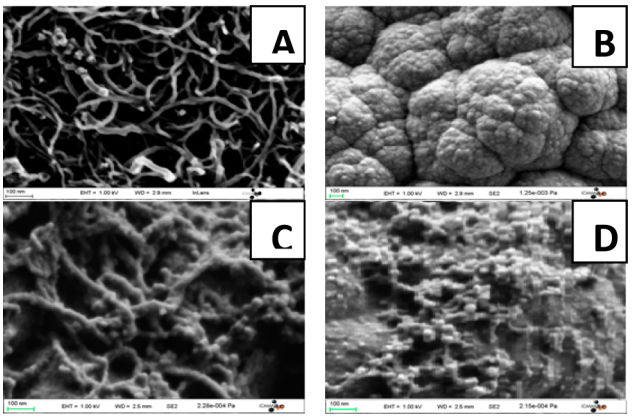

Figure 1. SEM images of gold surfaces covered by (A) carboxylated MWCNTs, (B) PPy, (C) MWCNTs-PPy, and (D) MWCNTs-PPy-PAMAM.

solution (Figure 1B).[27,28] The MWCNTs-PPy composite (Figure 1C) presents a dense structure of CNTs covered with polypyrrole film. Due to the presence of polypyrrole, the diameter of CNTs increased by about 10 nm when compared with SEM images of MWCNTs without polymer (Figure 1A). Modification of MWCNTs-PPy with PAMAM G4 leads to small nanoparticles deposited on the composite surface which confirms the attachment of the dendrimers (Figure 1D). The homogeneous distribution of PAMAM G4 dendrimers on the surface demonstrates high dispersion of these nanoparticles as the functionalization could occur on the entire nanomaterial surface. In the case of MWCNTs-PPy dipped in a solution of PAMAM G4 at open cell potential, no modification of the surface was observed. This confirms the electrodeposition of PAMAM G4 through oxidation of the amine groups, which are bonded covalently to the nanomaterial surface.

Molecular characterization were performed following FT-IR (see section S-2.3) and XPS analysis for the different surfaces: (a) carboxylated MWCNTs adsorbed on gold electrode, (b) MWCNTs-PPy, and (c) MWCNT-PPy-PAMAM. Because FT-IR analysis (see section S-2.3) did not allow to obtain clear and satisfactory results, XPS spectra could confirm in a reliable manner modifications of the aforementioned surfaces (MWCNTs, MWCNTs-PPy) with PAMAM G4. Figure 2 shows the results of XPS analysis in carbon and nitrogen regions for MWCNTs-PPy before and after PAMAM G4 electrodeposition. The XPS spectra of the carboxylated MWCNTs and MWCTs-PAMAM layers were recorded for comparison and are presented in the Supporting Information (see section S-2.4 and Figure S-2.4). The XPS spectrum in the carbon region of MWCNTs-PPy layer (Figure 2A) shows six maximum bands after fitting and peak separation. A band at 284.50 eV could be attributed to C−C or C−H bonds; band energy at 285.48 eV to C−C bonds of CNTs defects; 286.00 eV to C−N or C−O; 287.50 eV to C═N or C═O; 288.50 eV to COOH groups; and 291.34 eV to π species (see section S-2.4 and Table S-1). These results are in agreement with the spectrum obtained for the oxidized MWCNTs groups and are in accordance with results obtained in literature.[29] For the spectrum of carboxylated MWCNTs without PPy, the main C−C peak maximum is slightly shifted toward a lower energy (283.74 eV) because of negative charge of the CNTs (Figure S-4A). The spectrum obtained after PAMAM electrodeposition on the surface of MWCNTs-PPy layer shows a significant increase of the peak ratio corresponding to C−N and C═O bonds at 286.24 and 287.94 eV, respectively (Figure 2B).[30−32] This was also observed in the case of MWCNTs surface after electrodeposition of PAMAM (see section S-2.4 and Figure S-4C).

The significant modifications after PAMAM G4 dendrimers attachment were also observed in the nitrogen range. MWCNTs did not show the presence of nitrogen, however MWCNTs-PPy spectrum demonstrated two nitrogen peaks which belong to polypyrrole and come from the coating of

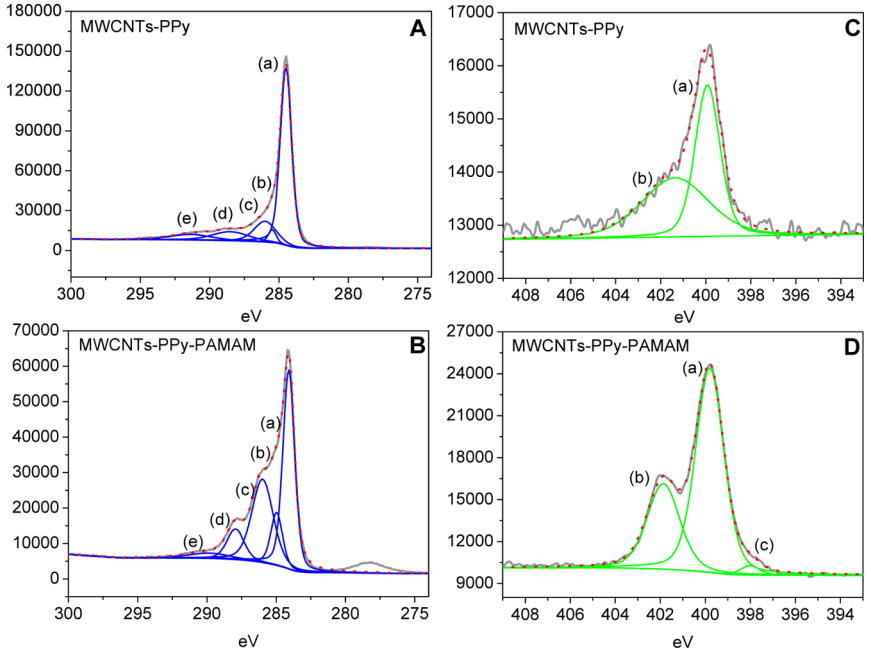

Figure 2. XPS spectra with fitting and peaks separation obtained in the carbon and nitrogen regions of MWCNTs-PPy layer (A, C) before and (B, D) after electro-oxidation of PAMAM G4 dendrimers.

DOI: 10.1021/acs.analchem.5b01761
Anal. Chem. XXXX, XXX, XXX−XXX

MWCNTs with a PPy film (Figure 2C). These peaks were fitted at 399.92 and 401.36 eV, which could be attributed to N−C or N−H bonds (peak a) and positively charged nitrogen ($-NH^+$ or $=NH^+$ (polaron/bipolaron)) (peak b), respectively.[32] Modification of the MWCNTs and MWCNTs-PPy surfaces with dendrimers were characterized with two nitrogen peaks at 399.80 and 401.86 eV, which could be attributed to amine and amide bonds respectively (Figure 2D). The peak at 399.80 eV could correspond to C−N and N−H bonds of aliphatic amines of covalently grafted to the surface PAMAM G4 dendrimers. The component of amide bond of PAMAM G4 is generally obtained at 400.5 eV[30,31] and XPS spectrum region 401−403 eV usually corresponds to positively charged nitrogen. In this nanocomposite, MWCNTs-PPy-PAMAM, the positive charge of amine was seen at 401.86 eV and this displacement could be caused by the attachment of PAMAM G4 to the highly conducting surface which results in a variation of binding energy value. These results confirm the association of PAMAM G4 dendrimers through covalent attachment to the nanocomposite layer and the presence of available amine groups for further functionalization.

Electron Transfer Characterization. The available amines on the surface of MWCNTs-PPy-PAMAM were linked with redox marker, ferrocene chemically modified with two activated phtalimydyl groups.[22,23] This modification allows attachment of ferrocene to amine groups of PAMAM G4 dendrimers leading to MWCNTs-PPy-PAMAM-Fc and then covalently link the ssDNA probe, according to the procedure described in Scheme 1. Association of ferrocenyl groups on the surface was studied with CV method. Figure 3A shows the CVs before and after bonding of ferrocene to the surface modified with MWCNTs-PPy-PAMAM. Once the covalent attachment of the redox marker was performed, the characteristic reversible redox signal of ferrocene was obtained, with oxidation and reduction peaks occurring at the same potential of 0.07 V (vs Ag/AgCl), as well as the oxidation and reduction current, as should be obtained for immobilized redox species. The resulting Faradaic current allows the surface coverage by ferrocenyl groups attached to MWCNTs-Py-PAMAM nanocomposite to be calculated, following the equation:[33]

$$\Gamma = \frac{Q}{nFA} \tag{1}$$

where Q is the charge under the cathodic or anodic wave, n is number of electrons involved in the redox process, F is the Faraday constant, and A is the area of the electrode. On the basis of eq 1, we calculated that the average surface coverage of ferrocene is 32 ± 2 nmol·cm^{-2}. These results agree with those obtained previously, where ferrocene was attached to MWCNTs-PAMAM, and PAMAM G4 were covalently grafted on MWCNTs through chemical attachment (38 ± 8 nmol·cm^{-2}).[20] The analysis of the redox signal within multiple scans shows high stability of the attached ferrocene and any decrease in current intensity is observed thanks to covalent attachment via amide link between the surface and redox marker.

The effect of scan rate on the redox signal was analyzed by varying scan rates from 0.005 to 10 V s^{-1}. An increase in redox current with variation of scan rate was observed (see section S-2.5 and Figure S-5). Both anodic and cathodic currents vary linearly with the scan rate (Figure S-5, lower inset). This demonstrates the surface-controlled process of charge transfer.[33] At relatively low scan rate (5 mVs^{-1}), the anodic and cathodic peak potentials remain at the same value, demonstrating the reversible redox process. At the highest scan rate (10 V s^{-1}), the anodic and cathodic peak potentials shift. The variation of the peak potentials was less than 0.2 V, indicating a significant rate of electron transfer. The electron transfer rate constant (k_s) can be determined using the equation developed by Laviron.[34] This method gives some indication in effective rate constant as it does not take into account some behavior occurs during redox process in complex redox system.

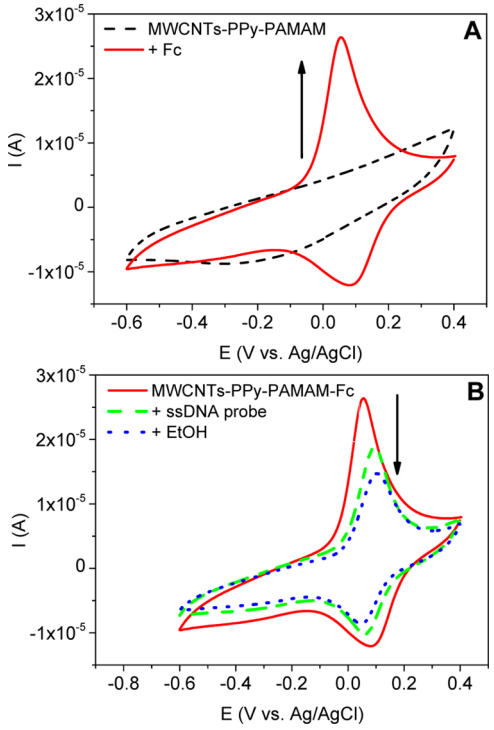

Figure 3. (A) Cyclic voltammograms of MWCNTs-PPy-PAMAM layer before and after attachment of ferrocenyl groups (Fc). (B) CV data obtained after each step of biosensor formation: MWCNTs-PAMAM-Fc (solid red line), MWCNTs-PAMAM-Fc-ssDNA (dashed green line), and MWCNTs-PAMAM-Fc-ssDNA-ethanolamine (dotted blue line). The CVs were recorded in 10 mM PBS solution at pH 7.4 with a scan rate of 50 mV s^{-1}.

$$m = \left(\frac{RT}{F}\right)\frac{k_s}{nv} \tag{2}$$

$$k_s = m\left(\frac{F}{RT}\right)nv \tag{3}$$

The value m was determined by adjustment of the curve $\Delta E_p = f(m^{-1})$ for an electron transfer coefficient $\alpha = 0.5$. The coefficient α was determined based on the variation in anodic potential ($E_{p,a} - E^0$) and cathodic potential ($E_{p,c} - E^0$) versus logarithm of the scan rate (Figure S-5, upper inset).

The effective k_s value obtained for MWCNTs-PPy-PAMAM-Fc was calculated as 13 ± 0.3 s^{-1}. Comparing the k_s obtained in the case of ferrocene attached to MWCNTs-PAMAM[20] or PPy-PAMAM,[21] where PAMAM dendrimers were linked through covalent reaction, the k_s were around 1.9 and 5.8 s^{-1}, respectively. Improvement was obtained when the attachment of PAMAM G4 was performed using electrochemical patterning method. In this case, the functionalization through electrochemical oxidation occurs across all of the CNTs surface, while chemical bonding occurs only at defects of nanotubes, where carboxylic groups are present. In this case the

DOI: 10.1021/acs.analchem.5b01761
Anal. Chem. XXXX, XXX, XXX−XXX

homogeneous distribution of ferrocene on the surface of CNTs improved the electron hopping between adjacent ferrocene centers.

Biolayer Formation and Synthetic DNA Detection. Biolayer construction involves covalent attachment of single-stranded DNA probes (ssDNA) modified with an amine group with 6 or 12 carbonyl spacer (C6 or C12 amino link), for synthetic DNA or PCR products determination, respectively. The ssDNA probe was covalently bonded to the ferrocene through an amide link. To avoid nonspecific adsorption, the biosensor surface was exposed to ethanolamine solution to saturate all unbound phtalymidyl esters of ferrocene.

The formation of the electrochemical biosensor was monitored by both cyclic voltammetry (CV) and square wave voltammetry (for SWV see section S-2.6 and Figure S-6) in PBS buffer (pH 7.4). Figure 3B shows the CVs performed after each step of biosensor construction showing a decrease of current after DNA attachment. This is related either to the low electron transfer or to the slow diffusion of ions to the surface during redox process, due to the attachment of large ssDNA molecules, as observed in previous work.[22,35]

Hybridization reactions were performed with two complementary targets: short chains of 15 bases (DNA_S) and long chains of 75 bases (DNA_L) containing complementary sequences to the DNA probe at end position. A wide range of concentrations (1 fM to 100 nM) of DNA targets were studied. The electrochemical detection of DNA targets was directly monitored by the ferrocene redox signal. Figure 4A exhibits the CV plots after hybridization with the DNA_S target in concentrations range from 1 fM to 100 nM. The redox current decreases within increasing of the DNA_S target concentrations. The same behavior was observed when DNA_L targets were incubated. SWV experiments, where the measured current corresponds only to faradic processes (Figure 4B), also demonstrated the same characteristics. An average attenuation of 77% on the intensity of oxidative current is obtained after hybridization with 100 nM of the DNA_S target. This suggests that almost all ferrocenyl groups immobilized on the surface were associated with the dsDNA.

On the basis of the changes of the current corresponding to the ferrocenyl groups redox signal obtained by SWV during detection of DNA_S and DNA_L targets, the calibration curves were plotted (Figure 4C, plot a and b). Hybridization of DNA_L target caused slightly higher current variations when compared to DNA_S. With the equal concentrations, large size of DNA affects more the redox signal. The same phenomenon was observed when DNA hybridization was performed with polypyrrole layers.[36]

Calibration curves plotted from these results exhibit a linear range of detection: from 1 fM to 10 pM for DNA_S and from 1 fM to 100 fM for DNA_L sensing (Figure 4C). On the basis of a signal-to-noise ratio (S/N) of 3 and taking the slope of the linear part of calibration curve, detection limits for both DNA targets were calculated as 0.3 fM. The reproducibility of the biosensors was tested with 4 independent measurements showing a relative standard deviation of 0.5−3.3%.

The nonspecific interactions were studied by incubating the biosensor with noncomplementary (nc) DNA targets bearing 14 bases (see section S-2.7). Figures S-7A and S-7B shows the result of CV and SWV analysis obtained after incubation of the sensor in a solution of DNA_S and nc DNA targets at same concentration of 1 μM. These results clearly show no variation in current after reaction with nc DNA target, while the incubation with complementary DNA_S caused a large variation. This demonstrates the high selectivity of the biosensors.

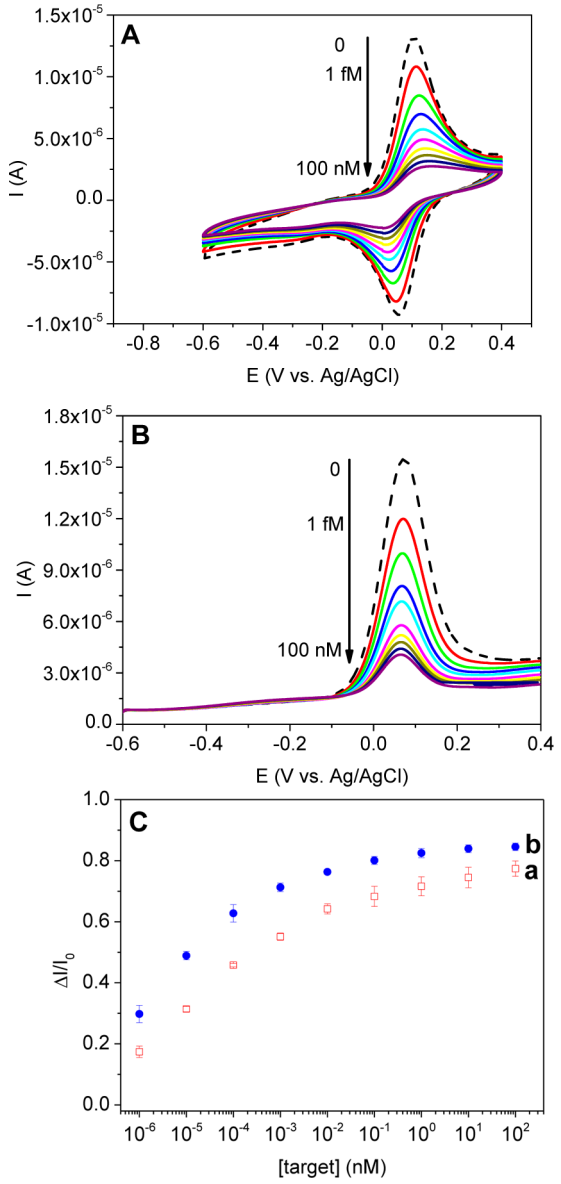

Figure 4. (A) CVs and (B) SWVs of biosensors after hybridization of complementary target DNA_S with single-stranded DNA probe at various concentration of targets (1 fM to 100 nM). CVs were recorded in PBS solution at pH 7.4 with a scan rate of 50 mV·s^{-1}, SWVs were recorded with a modulation amplitude of 20 mV, a frequency of 50 Hz and conditioning time of 180 s. (C) Plot of the relative changes of the current peak current versus concentration of (a) DNA_S target and (b) DNA_L target on the MWCNTs-PPy-PAMAM-Fc biosenor. $\Delta I = (I_0 - I)$, where I_0 is the peak of current prior to incubation with complementary target and I corresponds to the peak current after incubation of the sensor with different concentrations of tested target.

DNA Detection from Clinical Samples of Drug Resistant *Mycobacterium tuberculosis*. The biosensor was also applied for the detection of DNA from the pathogen agent of tuberculosis, *Mycobacterium tuberculosis* and was used to discriminate the single nucleotide polymorphism (SNP) T (TCG/TTG) conferring resistance of *M. tuberculosis* to rifampicin drug. The PCR products (called c PCR) were composed of DNA fragment of 411 bases length from *rpoB (beta subunit of the RNA polymerase)* gene containing punctual

DOI: 10.1021/acs.analchem.5b01761
Anal. Chem. XXXX, XXX, XXX−XXX

TTG mutation. As a negative control, wild-type sequence without TCG/TTG mutation was used (called nc PCR). The specific DNA probe from c PCR products was composed of 18 bases modified with amine group and 12 carbonyl spacer (C12 amino link) at the 5′ end position and was covalently attached to the biosensor surface via the amide link, following procedure as described in the experimental data. After a blocking step with ethanolamine, the hybridization reaction with either complementary sequence (c PCR) and the sample with the wild-type sequence (nc PCR) was performed. The biosensors were then analyzed using CV and SWV techniques and the results are demonstrated in Figures 5A and 5B. Hybridization reaction

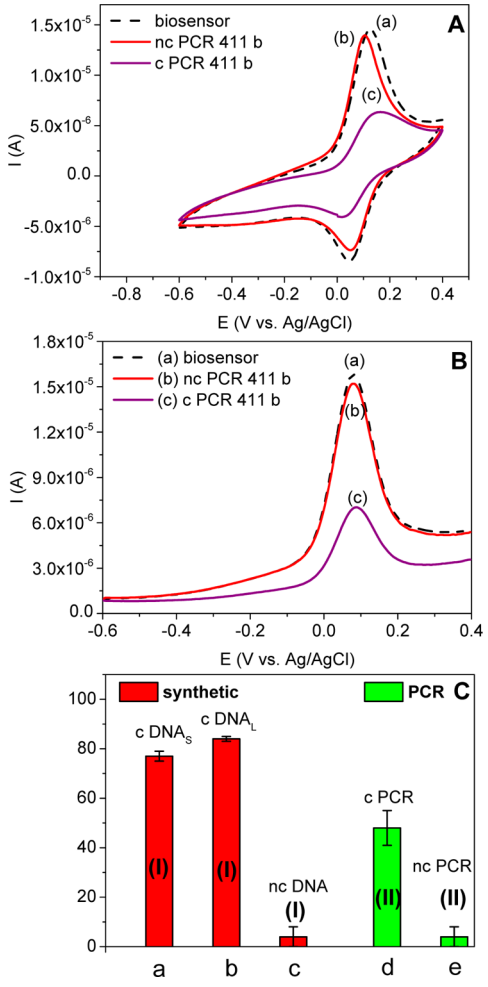

Figure 5. (A) CVs and (B) SWVs show detection of PCR products of 411 bases with (c PCR) and without (nc PCR) complementary sequence. (C) Histogram with summary of the results obtained during detection of synthetic DNA (system I, red bars) where (a) corresponds to sensing of the complementary DNA_S target of 15 bases, (b) DNA_L of 75 bases, (c) non complementary nc DNA target of 14 bases, as well as PCR samples (system II, green bars), where bar d corresponds to detection of complementary and bar e corresponds to noncomplementary PCR products of 411 bases.

with c PCR products leads to a change in the ferrocene redox current. The average variations in current were calculated as 48 ± 7% and were based on 5 independent measurements from different *M. tuberculosis* DNA clinical isolates. Incubation with the wild-type, nc PCR sample, resulted in small changes in current calculated as 4 ± 4%. These results are summarized in the form of a histogram (Figure 5C), where columns a, b, c (red bars) represent results obtained for the detection of synthetic DNA targets, while columns d and e (green bars) represent results for the detection of PCR products.

These results demonstrate that biosensors based on the MWCNTs-PPy-PAMAM-Fc composite, formed through electrochemical patterning was able to measure DNA from biological samples, such as DNA extracted from *Mycobacterium tuberculosis* strains. Moreover, such biosensor was characterized with high analytical performance allowing the distinction of SNP mutation. This method of detection could be generalized to any DNA target from a PCR product as the specific DNA probe is attached at the last step of biosensor assembly. The formation of such structure with electrochemical patterning leads to a homogeneous distribution of DNA target on the surface and also a functionalization of whole MWCNTs surface with PPy and PAMAM G4 layers. These properties allow obtaining high performance regarding DNA sensing and permit to avoid the nonspecific interaction of DNA with such surface.

This electrochemical biosensor was compared to some biosensors presented in literature where PCR products detection was demonstrated (see Table S-2). Although some sensors demonstrated efficient detection of DNA from PCR samples, this is the first time that biosensor based on electrochemical assembly of MWCNTs, PPy, and PAMAM G4 dendrimers has been shown to detect pathogenic DNA with SNP mutation through direct electrochemical measurement without further treatment. The easy formation of this biosensor beside their high reproducibility and very low time-consuming performed by chemical association of MWCNTs polypyrrole and PAMAM within electrochemical deposition place the present DNA sensor very highly competive for DNA sensing.

CONCLUSION

In this work, we reported a novel approach for highly sensitive amperometric detection of DNA with single nucleotide polymorphism mutation extracted from *M. tuberculosis*, based on the nanomaterial composed of MWCNTs coated with PPy, acting as a transducer and redox dendrimers amplifying the electrochemical signal. We demonstrated that encapsulation of MWCNTs with the PPy layer during polymerization process allows association of CNTs to the surface in a controlled and reproducible way. This MWCNTs-PPy conjugation increases the active surface area and improves the electrical properties of the layer. We demonstrated that the functionalization of the MWCNTs-PPy platform could be achieved through electro-oxidation of the amine groups of poly(amidoamine) dendrimers of fourth generation (PAMAM G4), which leads to their covalent attachment onto the modified surface. The key advantage of the PAMAM G4 association through electro-oxidation is demonstrated by the simplicity of this reaction, without the need of any prior chemical modifications. In addition, PAMAM G4 are present all across the composite surface as compared to chemical modifications of MWCNTs where molecules are present only at the edges of nanotubes. Improved electron transfer has been demonstrated compared to chemically modified surfaces, thanks to a homogeneous distribution of redox-active ferrocene bounded on the surface. The resultant MWCNTs-PPy-PAMAM-Fc layer was demonstrated as an efficient platform for DNA detection by monitoring the ferrocene redox marker. We have also shown that the binding of ssDNA targets to the surface resulted in a significant variation of redox currents, with very low detection limit of 0.3 fM. The biosensor has shown appreciably sensitivity

DOI: 10.1021/acs.analchem.5b01761
Anal. Chem. XXXX, XXX, XXX−XXX

and selectivity to real samples of DNA from *Mycobacterium tuberculosis*, demonstrating a potential in its application in DNA sensing and specific detection of single nucleotide polymorphism (SNP). Its potential application can concern pathogens diagnostic and drug resistance detection for therapeutic purpose or resistance surveillance.

■ ASSOCIATED CONTENT

Supporting Information

The Supporting Information is available free of charge on the ACS Publications website at DOI: 10.1021/acs.analchem.5b01761.

PCR products, reagents, instrumentation, characterization of MWCNTs-PPy layer, attachment of PAMAM G4 dendrimers, characterization of carboxylated MWCNTs, MWCNTs-PPy, and MWCNTs-PPy-PAMAM layers by FT-IR technique, characterization of carboxylated MWCNTs by XPS technique, before and after electro-oxidation of PAMAM G4 dendrimers, electrochemical characterization, biolayer formation monitored using square wave voltammetry (SWV) method, non-specific interactions, and comparison of PCR products detection by different biosensors (PDF)

■ AUTHOR INFORMATION

Corresponding Author

*Tel. +33-1-69157440. Fax: +33-1-69157281. E-mail: hafsa.korri-youssoufi@u-psud.fr.

Notes

The authors declare no competing financial interest.

■ REFERENCES

(1) Rivas, G. A.; Rubianes, M. D.; Rodrýguez, M. C.; Ferreyra, N. F.; Luque, G. L.; Pedano, M. L.; Miscoria, S. A.; Parrado, C. *Talanta* **2007**, *74*, 291−307.
(2) Ajayan, P. M. *Chem. Rev.* **1999**, *99*, 1787−1800.
(3) Wang, J.; Lin, Y. *TrAC, Trends Anal. Chem.* **2008**, *27*, 619−626.
(4) Ivanov, A. N.; Younusov, R. R.; Evtugyn, G. A.; Arduini, F.; Moscone, D.; Palleschi, G. *Talanta* **2011**, *85*, 216−211.
(5) Wang, Y.; Joshi, P. P.; Hobbs, K. L.; Johnson, M. B.; Schmidtke, D. L. *Langmuir* **2006**, *22*, 9776−9783.
(6) Lata, S.; Batra, B.; Kumar, P.; Pundir, C. S. *Anal. Biochem.* **2013**, *437*, 1−9.
(7) Hnaien, M.; Bourigua, S.; Bessueille, F.; Bausells, J.; Errachid, A.; Lagarde, F.; Jaffrezic-Renault, N. *Electrochim. Acta* **2011**, *56*, 10353−10358.
(8) Wang, S. G.; Wang, R.; Sellin, P. J.; Zhang, Q. *Biochem. Biophys. Res. Commun.* **2004**, *325*, 1433−1437.
(9) Wang, J.; Musameh, M. *Anal. Chim. Acta* **2005**, *539*, 209−213.
(10) Xu, Y.; Ye, X.; Yang, L.; He, P.; Fang, Y. *Electroanalysis* **2006**, *18*, 1471−1478.
(11) Chen, G. Z.; Shaffer, M. S. P.; Coleby, D.; Dixon, G.; Zhou, W.; Fray, D. J.; Windle, A. H. *Adv. Mater.* **2000**, *12*, 522−526.
(12) Hughes, M.; Chen, G. Z.; Shaffer, M. S. P.; Fray, D. J.; Windle, A. H. *Chem. Mater.* **2002**, *14*, 1610−1613.
(13) Zengin, H.; Zhou, W.; Jin, J.; Czerw, R.; Smith, D. W., Jr.; Echegoyen, L.; Carroll, D. L.; Foulger, S. H.; Ballato, J. *Adv. Mater.* **2002**, *14*, 1480−1483.
(14) Katz, E.; Willner, I. *ChemPhysChem* **2004**, *5*, 1084−1104.
(15) Caminade, A.-M.; Majoral, J.-P. *Chem. Soc. Rev.* **2010**, *39*, 2034−2047.
(16) Tsukruk, V. V.; Rinderspacher, F.; Bliznyuk, V. N. *Langmuir* **1997**, *13*, 2171−2176.
(17) Wei-Jie, S.; Shi-Yun, A.; Jin-Huan, L.; Lu-Sheng, Z. *Chin. J. Anal. Chem.* **2008**, *36*, 335−338.
(18) Zhu, N.; Gao, H.; Xu, Q.; Lin, Y.; Su, L.; Mao, L. *Biosens. Bioelectron.* **2010**, *25*, 1498−1503.
(19) Gao, H.; Jiang, X.; Dong, Y.-J.; Tang, W.-X.; Hou, C.; Zhu, N. N. *Biosens. Bioelectron.* **2013**, *48*, 210−215.
(20) Miodek, A.; Castillo, G.; Hianik, T.; Korri-Youssoufi, H. *Anal. Chem.* **2013**, *85*, 7704−7712.
(21) Miodek, A.; Castillo, G.; Hianik, T.; Korri-Youssoufi, H. *Biosens. Bioelectron.* **2014**, *56*, 104−111.
(22) Korri-Youssoufi, H.; Makrouf, B. *Synth. Met.* **2001**, *119*, 265−266.
(23) Miodek, A.; Sauriat-Dorizon, H.; Chevalier, C.; Delmas, B.; Vidic, J.; Korri-Youssoufi, H. *Biosens. Bioelectron.* **2014**, *59*, 6−13.
(24) Ghanem, M. A.; Chrétien, J. M.; Pinczewska, A.; Kilburn, J. D.; Bartlett, P. N. *J. Mater. Chem.* **2008**, *18*, 4917−4927.
(25) Chrétien, J. M.; Ghanem, M. A.; Bartlett, P. N.; Kilburn, J. D. *Chem. - Eur. J.* **2008**, *14*, 2548−2556.
(26) Zhang, L.; Jiang, X.; Wang, E.; Dong, S. *Biosens. Bioelectron.* **2005**, *21*, 337−345.
(27) Carquigny, S.; Segut, O.; Lakard, B.; Lallemand, F.; Fievet, P. *Synth. Met.* **2008**, *158*, 453−461.
(28) Patois, T.; Lakard, B.; Monney, S.; Roizard, X.; Fievet, P. *Synth. Met.* **2011**, *161*, 2498−2505.
(29) Datsyuk, V.; Kalyva, M.; Papagelis, K.; Parthenios, J.; Tasis, D.; Siokou, A.; Kallitsis, I.; Galiotis, C. *Carbon* **2008**, *46*, 833−840.
(30) Graf, N.; Yegen, E.; Gross, T.; Lippitz, A.; Weigel, W.; Krakert, S.; Terfort, A.; Unger, W. E. S. *Surf. Sci.* **2009**, *603*, 2849−2860.
(31) Nazarpoor, Z.; Ma, S.; Fanson, P. T.; Alexeev, O. S.; Amiridis, M. D. *Polym. Degrad. Stab.* **2012**, *97*, 439−451.
(32) Carquigny, S.; Sanchez, J.-B.; Berger, F.; Lakard, B.; Lallemand, F. *Talanta* **2009**, *78*, 199−206.
(33) Bard, A. J.; Faulkner, L. R. *Electrochemical Methods: Fundamentals and Applications*, 2nd ed.; Wiley: New York, 2001.
(34) Laviron, E. *J. Electroanal. Chem. Interfacial Electrochem.* **1979**, *101*, 19−28.
(35) Lê, H. Q. A.; Chebil, S.; Makrouf, B.; Sauriat-Dorizon, H.; Mandrand, B.; Korri-Youssoufi, H. *Talanta* **2010**, *81*, 1250−1257.
(36) Korri-Youssoufi, H.; Yassar, A. *Biomacromolecules* **2001**, *2*, 58−64.

DOI: 10.1021/acs.analchem.5b01761
Anal. Chem. XXXX, XXX, XXX−XXX